Tuning $Zr_{12}O_{22}$ Node Defects as Catalytic Sites in the Metal-Organic Framework hcp UiO-66

Xi Chen,[†] Yinghui Lyu,[†] Zhengyan Wang,[†] Xu Qiao,[†*] Bruce C. Gates,[‡*] Dong Yang[†*]

[†] College of Chemical Engineering, Nanjing Tech University, Nanjing, Jiangsu 21000, China

[‡] Department of Chemical Engineering, University of California, Davis, California 95616, United States

KEYWORDS: *Zr_{12} nodes, defects, μ_2-OH groups, metal organic frameworks, epoxide ring-opening, alcohols*

ABSTRACT: Defects in metal organic frameworks (MOFs) play important roles in MOF reactivity and catalysis. Now we report evidence of the reactivity and the quantitative characterization of the missing linker defects on the $Zr_{12}O_{22}$ nodes in the MOF **hcp** UiO-66 (these are paired Zr_6O_8 nodes bridged by OH groups) and those on the Zr_6O_8 nodes of the MOF UiO-66. The defect sites catalyze the ring-opening reactions of epoxides with alcohols, and new sites formed by removal of bridging OH groups on the $Zr_{12}O_{22}$ nodes also participate in the catalysis. The **hcp** UiO-66 was synthesized from UiO-66 as well as from molecular precursors, and under various synthesis conditions, the nodes incorporated acetate ligands where linkers were missing, with the numbers of these ligands controlled by the synthesis conditions. These ligands are inhibitors of the catalytic reactions, and their removal by reaction with, for example, methanol (to form, for example, methyl acetate) preceded catalysis on the defect sites. The former MOF incorporated more defect sites than the latter, correspondingly being a more active catalyst. The defect sites on the $Zr_{12}O_{22}$ nodes are 2–6 times more active per site than those on the isolated Zr_6O_8 nodes, with the bridging OH groups increasing the catalytic activity of the neighboring node defect sites because new sites are formed after removal of them. The results help point to way to design and control of catalytic sites on metal oxide-like MOF nodes by tuning of the number and reactivity of the defect sites.

INTRODUCTION

Among the most widely investigated metal organic frameworks (MOFs) are those that incorporate Zr_6O_8 (or Hf_6O_8) nodes connected by linkers terminated with carboxylate groups. These MOFs are exemplified by the UiO-66 family, which has drawn wide attention because some of them (e.g., UiO-66) offer the advantages of high stability, structural tunability, and high densities of reactive groups, all of which are important for potential applications as catalysts and catalyst supports. [1-3]

Ideally, each Zr_6O_8 node of UiO-66 would be bonded to 12 linkers, but the number is usually less, because components present in the MOF synthesis compete with the linker precursors for bonding sites on the nodes. Ligands on the nodes may include formate, formed from dimethylformamide (DMF) used as a solvent in the syntheses,[4, 5] and others, such as acetate, formed from modulators such as acetic acid used in the syntheses.[4, 6] Thus, these MOFs have defects associated with the node-bound ligands: these ligands may be removed to leave open bonding sites; they may be replaced by other ligands (such as those undergoing catalytic reactions); and they may be reactive themselves, possibly being parts of catalytic sites.[5, 7-11]

Defects in MOFs are commonly classified as missing linker or missing node defects, and some have been investigated thoroughly.[12-16] Researchers have developed a number of approaches to counting and understanding node defects and tuning them.[4, 5, 15] The performance of some MOF catalysts is correlated with the number of defects.[5, 7, 17]

A compelling advantage of MOFs is their tunability—to give crystalline materials having wide ranges of surface areas, pore dimensions, and reactivities. MOFs with Zr_6O_8 nodes have commonly been tuned by variation of the lengths and compositions of the linkers.[2] Recent work illustrates MOFs with layered pairs of Zr_6O_8 nodes bridged by 6 μ_2-OH groups (Figure 1).[18-21] These offer unexplored opportunities for tuning MOF properties by control of the defect sites.

The MOF **hcp** Hf-UiO-67, reported by Grey's group,[18] incorporates $Hf_{12}(\mu_3\text{-}O)_8(\mu_3\text{-}OH)_8(\mu\text{-}OH)_6$ nodes, but it lacks stability, being transformed under ambient conditions into a 2-D layered **hxl** phase. The similar MOF, **hcp** Zr-UiO-68, reported by Lin's group,[21] has not yet been assessed for its stability, but the comparable MOFs **hcp** Zr-UiO-66[22] and **hcp** Hf-UiO-66,[23] were found to maintain their structures for more than a year under ambient conditions.

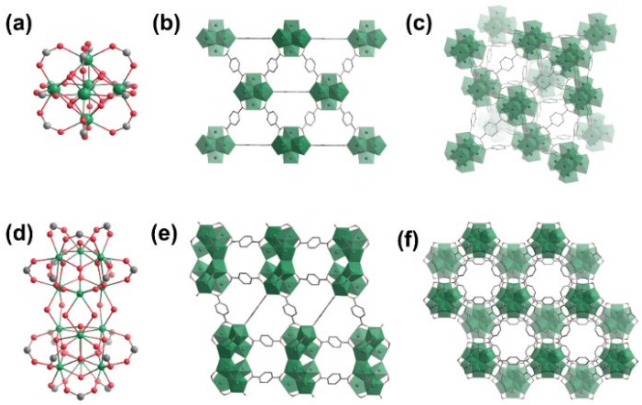

Figure 1. Structural representation of (a) $Zr_6O_4(\mu_3\text{-}OH)_4(COO)_{12}$ node (abbreviated as Zr_6O_8 node), (b) UiO-66 viewed from [101] direction, (c) UiO-66 viewed from [001] direction, (d) $Zr_{12}O_8(\mu_3\text{-}OH)_8(\mu_2\text{-}OH)_6(COO)_{18}$ node (abbreviated as $Zr_{12}O_{22}$ node), (e) **hcp** UiO-66 viewed from [100] direction, (f) **hcp** UiO-66 viewed from [001] direction.

We posit that more MOFs in this family that incorporate 12 Zr atoms per node will emerge and include some with various linkers, such as those reported for the related MOFs having 6 Zr atoms per node—and, further, that understanding and control of defects in these new MOFs might lead to the recognition of new ways to control MOF reactivity and catalytic properties. This subject has been largely overlooked, although it was recently addressed briefly by Grey's group.[23] They synthesized **hcp** Hf-UiO-66 from a solution of DMF, water, and formic acid, reporting NMR results showing that 26–47% of the node bonding sites were occupied not by linkers but rather by formate ligands, the number of which could be tuned by the amount of water used in the synthesis. This work raises questions about the reactivity and catalytic properties of the MOF. To address this topic, we focused on **hcp** Zr-UiO-66, synthesizing it separately from two precursors, $ZrOCl_2{\cdot}8H_2O$ and a MOF, UiO-66. We determined the stabilities of the samples with X-ray diffraction (XRD) crystallography and infrared (IR) spectroscopy, quantifying the defect sites (those occupied by acetate) by ^{1}H NMR spectroscopy of samples dissolved in aqueous NaOH + D_2O[4,5] and testing the MOFs as catalysts for ring-opening of epoxides with alcohols.

The results presented herein afford a comparison between the **hcp** Zr-UiO-66 samples and the UiO-66 from which some of these samples were made. They show that the transformation of UiO-66 to **hcp** UiO-66 in the presence of water and acetic acid yielded a more defective MOF than the sample made from $ZrOCl_2{\cdot}8H_2O$—and thereby a more active catalyst. The **hcp** UiO-66 was found to be less stable than UiO-66—undergoing dehydration resulting from removal of node μ_2-OH groups that ensued even at a temperature of only 230 °C. However, the data also demonstrate an advantage of the node μ_2-OH groups adjacent to defect sites—these defects facilitate the removal neighboring μ_2-OH groups (to make water) and thereby open new sites and thereby increase the catalytic activity.

RESULTS

Direct synthesis of hcp Zr-UiO-66 within a narrow operating window

In contrast to the synthesis of UiO-66 in the presence of DMF, the reported synthesis of **hcp** Zr-UiO-66 is done with a solution of acetic acid in water without DMF.[20,22] We varied the acetic acid:water ratio to elucidate the roles of these components, finding that **hcp** UiO-66 formed only when this ratio was 1:1 (volume). More water led to noncrystalline product, and more acetic acid led to a zirconium acetate characterized as of $Zr_6(O)_4(OH)_4(CH_3COO)_{12}$ (Figure 2).[24]

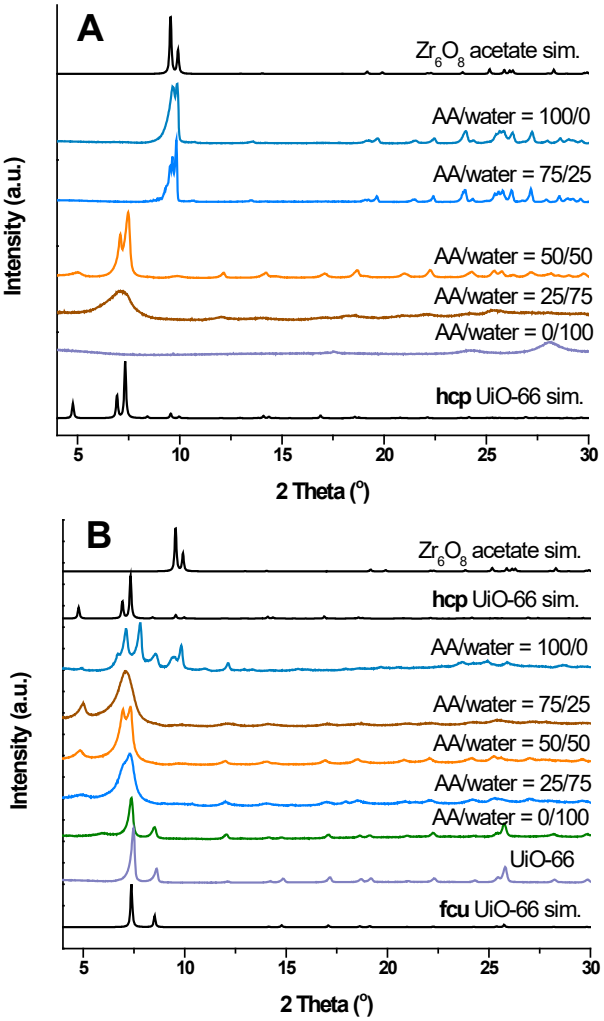

Figure 2. XRD patterns characterizing MOF samples synthesized from (A) $ZrOCl_2{\cdot}8H_2O$ and H_2BDC and (B) UiO-66 in the presence of solutions with various acetic acid (AA) and water volume ratios. H_2BDC is benzene-1,4-dicarboxylic acid.

Both components are clearly needed, water, evidently, to provide oxygen and/or hydrogen to form ligated Zr_6O_8 nodes (such as $Zr_6O_4(OH)_4$)[25] and, we infer, more important, to facilitate the formation of bridging μ_2-OH groups that help to stabilize the dimers of Zr_6O_8 nodes. Acetic acid was also essential, we infer—by virtue of the stabilization of the nodes by acetate ligands—by facilitating the MOF crystallization and hindering further aggregation in the presence of water.

To determine whether the solvent DMF that is crucial for the crystallization of UiO-66, of **hcp** Hf-UiO-66/UiO-67, and of **hcp** Zr-UiO-68[1,18,21,23] is also important for the synthesis of **hcp** Zr-UiO-66, we varied the concentrations of DMF, water, and acetic acid in the

synthesis of **hcp** Zr-UiO-66—finding, however, that none of the combinations led to a successful synthesis. We also used formic acid and benzoic acid as modulators in attempts to synthesize **hcp** Zr-UiO-66, but these experiments also failed to lead to synthesis of the MOF.

Determination of structures of MOFs and tuning of the node chemistries

To investigate the stability of **hcp** Zr-UiO-66, we did X-ray diffraction crystallography (XRD), finding that the MOF in air started losing crystallinity at 280 °C and collapsed at 400 °C (indicated by the disappearance of the 4.9° peak (Figure S1 in the SI). We emphasize that these are the first XRD data demonstrating the thermal stability of **hcp** Zr-UiO-66 and that they indicate that this MOF is not as stable as UiO-66. Thermogravimetric analysis (TGA) data (Figure S2, SI) show that the **hcp** Zr-UiO-66 was more dense than the ideal structure, consistent with the presence of water and with reported results.[23] The calculated number of water molecules per node was about 14, and we suggest that they were likely locked in the nest of bridging OH groups by hydrogen bonds and therefore difficult to remove by conventional activation at 150 °C under high vacuum. These results were bolstered by IR spectra (Figure S3, SI) including a broad band centered 3362 cm^{-1} and a band at 1656 cm^{-1} assigned to adsorbed water—which decreased in intensity as the temperature was ramped up. Yet a substantial amount of water was retained even when the temperature increased to 350 °C, indicating strong hydrogen bonding of the water molecules to the μ_2-OH groups. In contrast, physisorbed water in UiO-66 is readily desorbed under these conditions.[26] The properties of the bridging OH groups and the nests formed by them have not been explored before.

The intense IR band of hydrogen-bonded water almost swamped those of any hydroxyl groups of **hcp** UiO-66, but the latter could nonetheless be identified; the band characterizing μ_3-OH groups in **hcp** UiO-66 (Figure 3) was evident at 3674 cm^{-1}, matching the frequency of the equivalent band in the spectrum of UiO-66.[6] However, as the temperature was increased to 230 °C and then 250 °C, the peak split and shifted to 3686 cm^{-1} (Figure 3). Earlier work showed that the frequencies of bands characterizing the μ_3-OH groups are sensitive to the ligand environment of the Zr_6 node,[6] and the data (Figure 3) comparing the two MOFs reflect differences in the ligands on the nodes in the two MOFs. Taking these results together with the XRD results, we infer that removal of μ_2-OH groups by dehydration caused the IR band shifts and made the MOF less stable. Because the μ_2-OH groups were bonded directly to the nodes, the node structure lost its symmetry when these groups were partially removed.

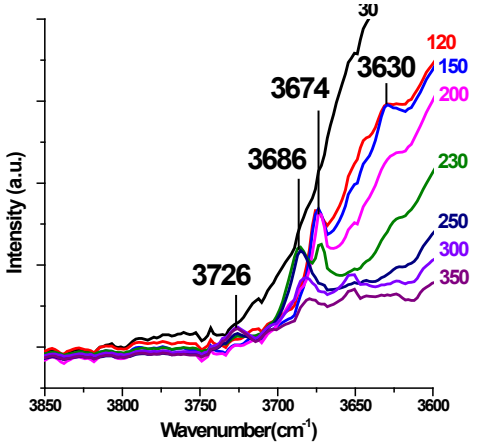

Figure 3. IR spectra in hydroxyl-group region characterizing **hcp** UiO-66 in flowing N_2 as the temperature was ramped from 30 to 350 °C. The colored numbers at the right represent temperatures in °C.

The μ_2-OH groups are close enough to each other to be hydrogen bonded, as shown by calculations at the level of density functional theory (DFT).[27] The 3630-cm^{-1} band is tentatively assigned to the hydrogen bonded species that link the OH groups, because it matches the trend calculated by DFT[27] and appears at lower frequencies than the μ_3-OH band. However, no single μ_2-OH IR band was observed at temperatures lower than 200 °C, although a band did appear at 3726 cm^{-1} upon partial dehydration of the sample at 230 °C, accompanied by a decrease in intensity of the 3630-cm^{-1} band. Thus, we infer that dehydration by reaction of μ_2-OH groups with each other started at a lower temperature (230 °C) than reaction of isolated μ_3-OH groups (~ 300 °C),[28] and the removal of μ_2-OH groups ultimately leads to the collapse of **hcp** UiO-66. We emphasize that the terminal OH groups suggested by Firth et al.[23] (with an IR band expected at about 3780 cm^{-1}, as reported for UiO-66[26]), were not evident for **hcp** UiO-66 in our experiments. A summary of the IR band assignments is given in Table 1.

Table 1. IR hydroxyl band assignments

MOF	IR band frequency, cm^{-1}	Assignment of band
UiO-66[a]	3780	terminal OH
	3674	μ_3-OH
hcp UiO-66[b]	3726	Single μ_2-OH
	3686	μ_3-OH (dehydrated node[c])
	3674	μ_3-OH
	3630-3650	hydrogen bonded μ_2-OH[d]

[a]as reported;[26] [b]this work; [c]partial dehydration by removal of μ_2-OH groups; [d]tentative assignment.

The tight window of conditions demonstrated by these results for synthesis of **hcp** Zr-UiO-66 evidently limits opportunities to tune its properties, including the number of defects. Thus, we were moti-

vated to take a different path forward and turned to the methods reported by Grey's group in converting Hf-UiO-66 to **hcp** Hf-UiO-66—which they carried out by adding increasing amounts of water in the transformation.[23] Thus, we attempted to convert UiO-66 into **hcp** UiO-66, with the former first synthesized as before with acetic acid as a modulator.[5,6] The structure was confirmed by XRD data to be **fcu** UiO-66 (Figure 2B). To initiate the desired transition, we treated the UiO-66 in a solution of acetic acid and water under conditions similar to those applied for synthesis of **hcp** UiO-66. Again, the acetic acid:water ratio was varied. The data demonstrate the high stability of UiO-66 in pure DI water at 150 °C. But when the reactant solution contained 25 vol% acetic acid, the UiO-66 was transformed, as shown by the XRD pattern indicating the disappearance of the **fcu** phase and the appearance of a new peak at 4.9° indicating the formation of **hcp** UiO-66. Further increases in the acetic acid concentration to 75 vol% led to increased formation of the **hcp** UiO-66. However, when pure acetic acid was used, a mixture of zirconium acetate ($Zr_6(O)_4(OH)_4(CH_3COO)_{12}$)[24] and poorly defined components formed.

These data show that both water and acetic acid are needed for the conversion of **fcu** UiO-66 to **hcp** UiO-66. We suggest that acetic acid played a role by breaking node–linker bonds and forming node–acetate bonds, presumably in reactions similar to those observed for reactions involving UiO-66 nodes and alcohols.[5] We emphasize that the water was necessary to trigger the dimerization of the Zr_6O_8 nodes and that, as a result of the transition from $Zr_6O_4(OH)_4(BDC)_6$ to $Zr_{12}O_8(OH)_{14}(BDC)_9$, some of the BDC linkers were removed, washed away with DMF in the subsequent synthesis steps.

For a further comparison, we chose **hcp** UiO-66 synthesized from $ZrOCl_2{\cdot}8H_2O$ and UiO-66 made with the same acetic acid:water ratio of 1:1, labeling the samples **hcp** UiO-66 and **hcp** UiO-66T (where T refers to the transition from UiO-66), respectively. Further, we compared the results with those obtained with UiO-66 (the parent for the synthesis of **hcp** UiO-66T) and with MOF-808,[29] because these MOFs both have Zr_6O_8 nodes but different numbers of defects per node and different pore apertures and diameters.[1,29]

The two **hcp** UiO-66 samples were found to have similar N_2 uptakes and BET surface areas, but the values were both lower than those characterizing UiO-66 and much lower than those characterizing MOF-808 (Table 2, Figure S6 in SI). The trend is consistent with reported data[22] that have been explained by the higher MOF density associated with the $Zr_{12}O_{22}$ cluster than with the Zr_6O_8 cluster. Pore size distributions were calculated by a DFT method and are shown in Figure S6B, SI. UiO-66 had a major pore with a diameter of 9.3 Å and two large pores, with diameters of 12.7 and 14.8 Å. We have suggested that the large pores are associated with defects,[6] and possibly missing linker and missing node defects, respectively, because larger pores are expected for defective structures, and pore sizes associated with missing node defects are also expected to be larger than those associated with missing linker defects. **hcp** UiO-66 and **hcp** UiO-66T were found to have major pores with diameters of 8.6 Å, which are smaller than those in UiO-66. The larger pores appeared at 12.7 and 14.8 Å for **hcp** UiO-66 and at 11.8 Å and 14.8 Å for **hcp** UiO-66T, and we associate these with missing linker and missing node defects, respectively. Further, dV/dD values characterizing these pores (V is volume, D is diameter) indicate that **hcp** UiO-66 has fewer defects, specifically missing linkers, than **hcp** UiO-66T. As expected,[29] MOF-808 has larger pores, with a maximum at a diameter of 17.1 Å.

TGA data characterizing the MOFs determined the number of defects per UiO-66 node to be 1.4 , as before,[6] but we could not determine comparable results for the other MOFs by TGA because of their low stabilities. We instead quantified the numbers of defects and ligands on the MOF nodes by using ^{1}H NMR spectroscopy of digested samples, as before[5,6] (Table 2). The data show that, per node, UiO-66 had 0.73 acetate ligands (from the modulator) and 0.29 formate ligands (formed by decomposition of DMF),[5] giving a total of 1.02 defect sites, consistent with reported results.[6] The **hcp** UiO-66 and **hcp** UiO-66T had only acetate and not formate ligands on the node defects because they were synthesized in acetic acid and water without DMF. Moreover, we exclude the possibility of terminal OH groups as ligands on node defects of our **hcp** UiO-66 samples, because the IR spectra do not include bands characteristic of such species. The results also demonstrate that **hcp** UiO-66T has more defect sites per node than hcp UiO-66, a result that is consistent with the pore size distribution data.

Taken together, the data demonstrate a methodology for tuning the number of defects on the $Zr_{12}O_{22}$ nodes and the viability of obtaining a relatively high density of defect sites on these nodes by using UiO-66 as precursor in the MOF synthesis. For comparison, the data show that MOF-808 incorporated 5.35 formate ligands per node, in agreement with its structure, $Zr_6O_5(OH)_3(BTC)_2(HCOO)_5(H_2O)_2$, determined by Yaghi's group.[29] We emphasize the total number of defects per node of MOF-808 was 6 (a value determined by its crystal structure), and the remaining 0.65 defects are inferred to have been occupied by water molecules, which are not identifiable in our ^{1}H NMR spectroscopy experiments.[6] The structures of the defects in these MOFs are summarized in Figure 4.

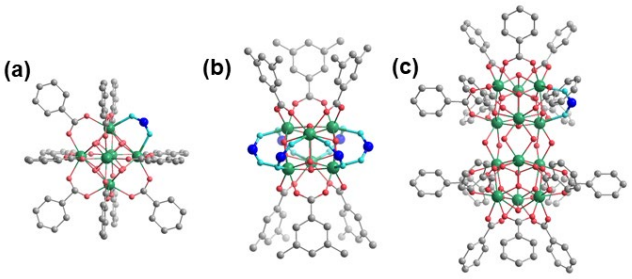

Figure 4. Illustration of missing-linker defects on Zr_6O_8 nodes of (a) UiO-66 and (b) MOF-808 and (c)$Zr_{12}O_{22}$ nodes of **hcp** UiO-66. Ligands on defects are highlighted in blue.

Table 2. Data characterizing the MOFs: N_2 adsorption isotherms, numbers of nonlinker ligands per MOF node determined by ^{1}H NMR spectroscopy, and catalytic performance for ring-opening reaction of propylene oxide by methylation.

Sample	Node	Linker pre-cursor[a]	N_2 adsorption isotherms		Number of nonlinker ligands determined by ^{1}H NMR spectroscopy			Catalyst performance[c]				
			BET surface area (m^2/g)	Diameters of pores (Å) [b]	formate ligands per node	acetate ligands per node	total of nonlinker ligands per node	Conversion (%)	Selectivity A (%)	Selectivity B (%)	TON[d]	TOF[d] (min^{-1})
UiO-66	$Zr_6O_4(OH)_4$	BDC	1327.6	9.3, 12.7, 14.8	0.29	0.73	1.02	11.9	64.0	36.0	6.7	0.0093
MOF-808	$Zr_6O_5(OH)_3$	BTC	1590.5	17.1	5.35		6.00	50.3	60.6	39.4	6.6	0.0092
hcp UiO-66	$Zr_{12}O_8(OH)_{14}$	BDC	709.5	8.6, 12.7, 14.8		1.43	1.43	37.1	82.3	17.7	37.9	0.053
hcp UiO-66T	$Zr_{12}O_8(OH)_{14}$	BDC	672.3	8.6, 11.8, 14.8		2.48	2.48	57.1	58.6	41.4	35.4	0.049
Blank								4.7	79.4	20.6		

[a]BDC is benzene-1,4-dicarboxylic acid; BTC is benzene-1,3,5-tricarboxylic acid. [b]Calculated by a DFT method. [c]Reaction conditions: propylene oxide 20 µL (0.29 mmol), methanol 1.0 mL (24.7 mmol), MOF catalyst 5.0 mg, temperature 55 °C. [d]Conversions determined in the blank experiments were subtracted for calculation of the TON and TOF values.

Probing MOF defect sites with a catalytic test reaction: ring-opening of epoxides with alcohols

As a further test of the reactivities of the MOFs, we used them as catalysts for ring-opening reactions of epoxides with alcohols. The test reactions were chosen because (1) they take place at low temperatures and pressures (e.g., 55 °C and 1 bar), ensuring the stability of the MOFs;[30, 31] (2) patterns of reactivity can be elucidated in experiments with families of alcohols and epoxides; and (3) these reactions have been shown to be catalyzed by defects in MOFs.[17]

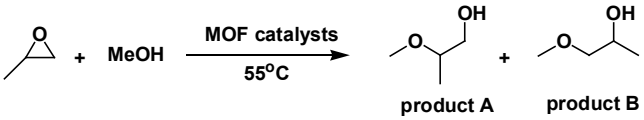

Scheme 1. Ring-opening reaction of propylene oxide with methanol catalyzed by the MOFs investigated in this work.

We first tested the catalytic reaction of propylene oxide with methanol (Scheme 1, Table 2). MOF-808 was found to have a higher activity (measured by conversion) than UiO-66—consistent with its six-fold higher number of defect sites per node. However, the catalytic properties calculated as TON (number of turnovers) and TOF (turnover frequency—rate per defect site) were almost the same for these two MOFs. Our results are consistent with reported results[17] and support the conclusion that the reaction was catalyzed by defect sites on the Zr_6O_8 nodes.[17] Similarly, the activity of **hcp** UiO-66T measured by conversion was found to be higher than that of **hcp** UiO-66, consistent with its higher density of defect sites, but again the reaction rates per defect site (TOF) were nearly the same (Table 2). More important, however, our results show that defect sites on the $Zr_{12}O_{22}$ nodes are markedly more active than the defect sites on Zr_6O_8 nodes—as indicated by the fivefold difference in TOF values (Table 2).

To generalize these catalytic results, we investigated a family of ring-opening reactions involving pairs of reactants selected from among two epoxides (propylene oxide and styrene oxide) and five alcohols (methanol, ethanol, isopropanol, isobutanol, and *tert*-butyl alcohol). The catalyst performance data (Table S3, SI) bear out the trends stated above—showing that defect sites on $Zr_{12}O_{22}$ nodes are 2–6 times more active (have higher TOF values) than defect sites on Zr_6O_8 nodes.

The data in Table 2 and Table S3 in the SI show general trends indicating that the activity of each of the MOF catalysts in the reaction with a given epoxide decreased as the reactant alcohol became larger, and styrene oxide was characterized by a higher reactivity than propylene oxide for each reaction partner.

Each alcohol–epoxide reaction gave two products, the primary alcohol (A) and the secondary alcohol (B), and the selectivities for product A were always higher than those for product B. The data also show that the selectivities for the two products were not controlled by the alcohols, but rather by the substituent on the epoxide, with styrene oxide being more selective for product A than propylene oxide.

Catalytically active sites on MOF nodes

To gain insight into the chemistry of the catalytic sites on the nodes, we used IR spectroscopy to monitor the UiO-66 and **hcp** UiO-66 as each reacted with either methanol or propylene oxide.

IR data (Figure S4, SI) indicate that methanol vapor at 1 bar was almost unreactive with UiO-66 at 55 °C when formate ligands (with a $\nu_{C\text{-}O} + \delta_{C\text{-}H}$ band at 2745 cm^{-1}) were present on the MOF node defects. However, at 150 °C, significant reaction took place, with formate being replaced by monodentate methoxy ligands (characterized by $\nu_{C\text{-}H}$ bands at 2931 and 2827 cm^{-1} and a $\nu_{C\text{-}O}$ band at 1157 cm^{-1}). The reaction forms methyl formate as a desorption product, identified by gas chromatography (Figure S13, SI). These results are consistent with our previous results.[5] We note that methoxy was bonded to the node defects of UiO-66 entirely as monodentate, but not bidentate, ligands. DFT calculations in our previous work[26] demonstrated that the former species has much lower free energy than the latter and is a favored bonding species on defect sites of UiO-66. The reaction that we infer is shown in Scheme 2.

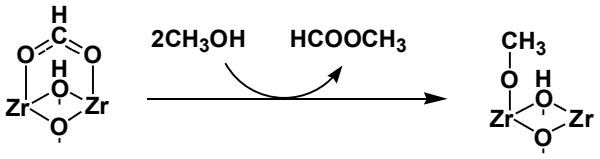

Scheme 2. Reaction of methanol with formate ligands on a node defect of UiO-66. The reaction between methanol and acetate ligands is suggested to proceed equivalently, with methyl acetate as a product.

Further, the IR data (Figure S4, SI) show that methanol is more reactive with $Zr_{12}O_{22}$ nodes of **hcp** UiO-66 than with Zr_6O_8 nodes of UiO-66 at 55 °C, as the reaction is characterized by the appearance of *bidentate* methoxy ligands indicated by the spectrum of the former (characterized by $\nu_{C\text{-}H}$ bands at 2925 and 2816 cm^{-1} and a $\nu_{C\text{-}O}$ band at 1031 cm^{-1}), but not the latter MOF. (Bidentate methoxy ligands on bulk ZrO_2 have been reported,[32] characterized by $\nu_{C\text{-}H}$ bands at 2923 and 2817 cm^{-1} and a $\nu_{C\text{-}O}$ band at 1032 cm^{-1}, close to the values observed here.) The data are consistent with the inference that these new bidentate methoxy ligands were not present on the node defects that accommodate only monodentate methoxy ligands. Therefore, we infer that these bidentate ligands must have been bonded on different sites—site present on $Zr_{12}O_{22}$ nodes but not on Zr_6O_8 nodes—and thus we suggest that the bidentate methoxy ligands formed in the reaction of methanol with μ_2-OH groups on the $Zr_{12}O_{22}$ nodes—that is, OH groups bridging individual Zr_6 nodes. Consistent with the suggestion of the replacement of hydrogen-bonded μ_2-OH groups by bidentate methoxy, the intensity of the 3650-cm^{-1} band decreased during the reaction with methanol. The results demonstrate that methanol is more reactive with μ_2-OH groups than with formate or acetate ligands on node defects at 55 °C.

Although the reaction between methanol and acetate ligands on defects of **hcp** UiO-66 nodes did not occur measurably in our experiments at 55 °C (consistent with what was observed with UiO-66), that reaction did occur as the temperature was increased to 150 °C. Thus, the band at 1157 cm^{-1} increased in intensity, indicating the formation of monodentate methoxy ligands on defect sites, replacing acetate, and the desorption product was identified by gas chromatography as methyl acetate (Figure S13, SI).

In summary, the data show that methanol reacts with formate and acetate on defect sites to form monodentate ligands on those sites and, separately, methanol reacts with μ_2-OH groups (which are present in MOFs with $Zr_{12}O_{22}$ nodes but not in MOFs with isolated Zr_6O_8 nodes) to form bidentate methoxy ligands.

Evidently, the reaction is selective, with methoxy ligands formed only on Lewis acid metal sites (with methoxy ligands are bonded directly to Zr atoms), but not reacting directly with Brønsted acid hydroxyl sites (μ_3-OH or μ_2-OH groups) to form bonds with them.

In contrast to methanol, propylene oxide was found to be highly reactive with μ_3-OH or formate ligands on the nodes of UiO-66 and **hcp** UiO-66 at 55 °C (Figure S5, SI). IR bands representing these latter species either disappeared or were significantly decreased in intensity after exposure of the sample to propylene oxide. As a result of the reaction, the propylene oxide ring opened, evidenced by the appearance of a band at 1046 cm^{-1}, which matches the $\nu_{C\text{-}O}$ band of propylene glycol.[33] It is clear from the data that propylene oxide is more reactive than methanol with the MOF nodes; however, the reactions are not selective, as propylene oxide reacts at both Lewis acid metal sites (indicated by the reaction with formate ligands) and Brønsted acid hydroxyl sites (indicated by the reaction with μ_3-OH groups); details of the chemistry remain to be elucidated.

To determine the number of node sites that can be occupied by methoxy ligands, we treated each of the three MOFs, UiO-66, **hcp** UiO-66, and **hcp** UiO-66T, with methanol vapor at 1 bar and 150 °C for 24 h to allow the complete replacement of the reactive formate or acetate ligands (or μ_2-OH groups when they were present) with methoxy ligands, and then held each sample under high vacuum for 12 h to remove any physisorbed methanol. Further XRD experiments showed that these three MOFs were all stable under the treatment conditions, but when the comparable experiments were done with MOF-808, the data showed that it was not stable.

To determine the number of methoxy ligands on each of the MOFs after exposure to methanol, we used ^{1}H NMR spectroscopy of the digested samples. The data give no evidence of formate or acetate, confirming that these ligands had been fully removed in the methanol treatments. The data further show that these groups had been replaced with methoxy (Figures S9-S11 in SI). Specifically, they show that UiO-66, **hcp** UiO-66, and **hcp** UiO-66T incorporated 0.90, 4.40, and 7.67 methoxy ligands per node, respectively. The number of methoxy ligands on UiO-66 is close to the total number of formate and acetate ligands in the original sample (1.02). Thus, it is clear that, in UiO-66, each node defect bonded to only one methoxy group, a result that is consistent with our previous results.[5] In contrast—and consistent with the results stated above related to the reactivity of the bridging OH groups, the data show that the numbers of methoxy ligands on **hcp** UiO-66 and on **hcp** UiO-66T after the methanol treatment were about 3.1-fold greater than the numbers of defects determined originally by the node occupancy by acetate ligands. On the basis of this difference, we thus reinforce the inference stated above that methanol reacted not only to replace the acetate ligands on defect sites, but it also reacted with other groups on the nodes that we identified as μ_2-OH groups, in agreement with the IR data. The quantitative results determined in the NMR experiments provide additional important information: they show that not all of the μ_2-OH groups are reactive with methanol, because the numbers of these ligands that were replaced after the methanol treatment were 2.97 and 5.19 per node for **hcp** UiO-66 and **hcp** UiO-66T, respectively, but the total number of this ligands per node is six (as determined by the crystal structure of **hcp** UiO-66). The results show that only about two μ_2-OH groups per defect site can be replaced by methoxy ligands, thus we infer that they are adjacent to defect sites.

A simplified representation of this chemistry involving methanol and formate ligands on the nodes (including μ_2-OH groups) is suggested in Scheme 3. This chemistry is consistent with all our observations, but we recognize that there is more to learn about it.

We suggest a rough comparison between the reactivity of the μ_2-OH groups on the nodes with the reactivity of some OH groups bonded to Zr atoms on bulk zirconia.[32] We suggest that an explanation for the high reactivity of μ_2-OH groups adjacent to defect sites on the nodes is that these μ_2-OH groups may be bonded to coordinatively unsaturated Zr atoms which are created on defect sites after replacement of formate or acetate ligands with monodentate methoxy ligands (Scheme 3(1)).

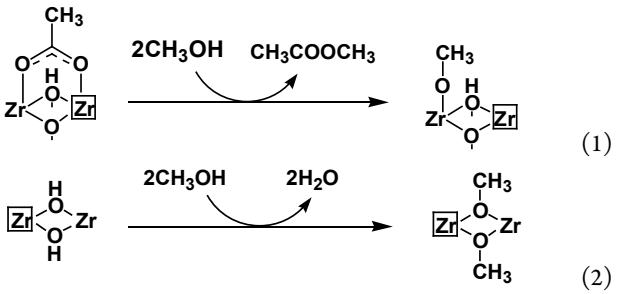

Scheme 3. Schematic representation of reactions on $Zr_{12}O_{22}$ nodes of **hcp** UiO-66 involving methanol and acetate ligands on a node defect (1) and with μ_2-OH groups bonded to a node defect (2). Zr in squares represents the node Zr atoms that before reaction with methanol are associated with both defect sites and μ_2-OH ligands.

Thus, the higher catalytic activities of the defect sites in **hcp** UiO-66 and **hcp** UiO-66T than of those in UiO-66 (i.e., the higher TOF of the former MOF) are attributed to the replacement of μ_2-OH groups neighboring these defect sites by methoxy ligands and thereby the creation of more sites where the reactants in the catalytic reaction can be converted. That is, the number of μ_2-OH groups that can be replaced for reaction is determined by the number of defects—the number of sites where acetate ligands initially reside.

DISCUSSION

Reaction chemistry on the MOF nodes

To clarify, defect sites as we use the term here refer to non-linker-bonded node sites to which formate, acetate, or methoxy ligands can be bonded (as shown in Schemes 2 and 3(1)), but they do not include those sites formed by replacement of μ_2-OH groups (Scheme 3(2)). We recognize that this usage of the term "defect sites" should not be considered to be general. There is more to do to elucidate the structures and reactivities of sites on MOF nodes.

The data demonstrate that the active sites for epoxide ring-opening reactions on $Zr_{12}O_{22}$ nodes of **hcp** UiO-66 are opened defect sites—that is, those after removal of the initially present formate and acetate ligands, as well as newly opened sites formed by removal of the adjacent μ_2-OH groups, approximately two of them. We emphasize that the initial ligands on defect sites and their adjacent μ_2-OH groups are inhibitors of the catalytic reactions and must be removed before the sites become active in catalysis. These inhibitors can be removed by reactions with either alcohols or epoxides to open the catalytically active sites. These sites can be readily probed with methanol because of the favorable chemistry of the reactions between methanol and the species initially bonded to the node sites. It is helpful for elucidation of the chemistry that the bonding of methoxy ligands is rather well understood.

We infer that the μ_2-OH groups do not themselves catalyze the reactions—if they alone were the catalytic groups, then the TOFs would not be related to the number of defects—and the data show that they are. Further weighing against the likelihood that the μ_2-OH groups are the catalytically active species is the result that the μ_3-OH groups were found to have the same frequency for **hcp** UiO-66 and UiO-66 (3674 cm^{-1}, Table 1), implying that there were no significant electronic effects of the μ_2-OH groups on node defects, as would be expected if they were the catalytic species. Moreover, any significant synergy between μ_2-OH groups and catalytic sites for accelerating the reactions is inferred not to be significant, because the TOF values (rates per defect site) characterizing $Zr_{12}O_{22}$ nodes (where μ_2-OH groups reside) are 2–6 times greater than those of the Zr_6O_8 nodes, and the former represent sites that are approximately threefold more active than the latter.

Because the ring-opening reactions were catalyzed by defect sites where both methanol and propylene oxide can bond (but not by hydroxyl groups, where propylene oxide but not the coreactant alcohol apparently can bond), we infer that the catalytic reaction proceeds through a Langmuir-Hinshelwood mechanism, whereby both reactants are bonded to each active node—on neighboring sites.

Further, the product A has been inferred to form by an S_N1 mechanism through a carbocation intermediate.[34] We infer that the acid sites (likely Lewis acid sites) on node defects first activate an epoxide to form a secondary carbocation that is further attacked by adsorbed methanol/methoxy, ultimately leading to product A. Product B is suggested to form in an S_N2 mechanism, by which the adsorbed methanol/methoxy attacks adsorbed epoxides on the primary carbon side to open the ring and form product B.

For all the reactions tested here, the S_N1 mechanism giving product A is favored over the S_N2 mechanism, with selectivities controlled by the epoxide rather than the alcohol. The benzene ring of styrene oxide can donate more electron density than the methyl group of propylene oxide, which helps to stabilize the intermediate carbocation, and, as a result, both reaction rates and selectivities to product A are significantly higher for reactions with styrene oxide than those with propylene oxide.

The catalytic activities were also found to be influenced by the size of the alcohol. As the substituents on the alcohol become larger and bulkier, the steric hindrance to the adsorption of alcohols on the active sites evidently becomes greater, and so the activities decrease significantly.

Controlling microenvironments of MOF nodes

Promotional effects of substituents on the BDC linkers of UiO-66 have been reported numerous times. One investigation[35] showed that incorporation of Br groups on BDC linkers in UiO-66 markedly increased the catalytic activity for styrene oxide ring opening in the reaction with methanol, but the mechanism was not fully elucidated. NO_2 ligands on BDC linkers in UiO-66 markedly increased the catalytic activity for cyclization of citronellal[7] and the activity for the reduction of 4-*tert*-butylcyclohexanone with isopropanol[36]–with both reactions catalyzed by defects. The strong electron-withdrawing effect of the NO_2 ligands on the nodes was invoked to explain the high activity of the modified UiO-66. In another example, NH_2 ligands on the BDC linkers of UiO-66 markedly increased the rate of the catalytic hydrolysis reaction of nerve agent simulants,[37] and recent results[38] demonstrated that these groups controlled the microsolvation environment of the Zr_6O_8 node defect sites, thereby increasing the rates.

Further, adjacent node defect sites were inferred to be the active sites for ethanol dehydration to give diethyl ether—an inference bolstered by DFT calculations showing that the activation enthalpy of the reaction on these sites was much lower than that characterizing reaction on single defect sites.[5]

These examples illustrate various roles of groups on MOF nodes in the UiO family influencing catalytic performance. The results reported here illustrate a different and heretofore undiscovered effect of groups on the MOF nodes, showing that hydroxyl ligands adjacent to node defect sites can be selectively removed by reaction with reactant methanol and thereby open new sites to facilitate catalytic reaction on the node defect sites. Taken together, these examples demonstrate a broad, emerging set of opportunities for controlling the microenvironments of MOF nodes to tune catalytic performance. There are rich prospects for the design of catalytic sites in the well-defined structures of MOFs.

CONCLUSIONS

The MOF **hcp** UiO-66, incorporating $Zr_{12}O_{22}$ nodes, was synthesized in a solution of acetic acid and water by using either $ZrOCl_2{\cdot}8H_2O$ or UiO-66 as precursor. Acetic acid and water were both found to be essential for the synthesis. The MOF was found to be less stable than UiO-66 because of dehydration resulting from reaction of μ_2-OH groups with each other, which took place at 230 °C. **hcp** UiO-66 formed from UiO-66 was found to incorporate more defect sites than that synthesized from $ZrOCl_2{\cdot}8H_2O$, and these sites were found to be important for catalysis of ring-opening epoxidation reactions with alcohols, with the data implying that the reactions on defect sites of the $Zr_{12}O_{22}$ nodes were increased markedly when new open sites were created by the removal of neighboring μ_2-OH groups by reaction with methanol. We anticipate that the new chemistry of hydroxyls and defect sites on the nodes will provide new opportunities for design of MOF catalysts and that the opportunities for such subtle control of the chemistry will be richer for structurally well-de-

fined metal oxide-like nodes on MOFs than for intrinsically heterogeneous bulk metal oxides.

AUTHOR INFORMATION

Corresponding Author

*dyang@njtech.edu.cn

*bcgates@ucdavis.edu

*qct@njtech.edu.cn

ORCID

Dong Yang: 0000-0002-3109-0964
Bruce C. Gates: 0000-0003-0274-4882

Notes

The authors declare no completing financial interest.

ASSOCIATED CONTENT

Supporting Information. Experimental details are reported, primarily MOF synthesis, XRD patterns, TGA data, IR spectra, ^{1}H NMR spectra, N_2 isotherms, SEM images, desorption data, and catalyst performance data. This material is available free of charge via the Internet at http://pubs.acs.org.

ACKNOWLEDGMENTS

D.Y. thanks the "Distinguished Professor" program (2018) and the "Innovative and Entrepreneurial Talent" program (2019) of Jiangsu province and the Priority Academic Program Development of Jiangsu Higher Education Institutions (PAPD) for funding this research. The work at the University of California was supported by the Inorganometallic Catalyst Design Center, a U.S. Department of Energy Basic Energy Sciences-funded Energy Frontier Research Centers (grant DE-SC0012702). We thank Prof. Chongqing Wang of Nanjing Tech University for helping with the XRD measurements and Prof. Jun Yu of Shanghai Institute of Technology for helping with the IR measurements.

REFERENCES

(1) Cavka, J. H.; Jakobsen, S.; Olsbye, U.; Guillou, N.; Lamberti, C.; Bordiga, S.; Lillerud, K. P., A new Zirconium Inorganic Building Brick Forming Metal Organic Frameworks with Exceptional Stability. *J. Am. Chem. Soc.* **2008,** *130*, 13850-13851.

(2) Bai, Y.; Dou, Y. B.; Xie, L. H.; Rutledge, W.; Li, J. R.; Zhou, H. C., Zr-Based Metal-Organic Frameworks: Design, Synthesis, Structure, and Applications. *Chem. Soc. Rev.* **2016,** *45*, 2327-2367.

(3) Yang, D.; Gates, B. C., Catalysis by Metal Organic Frameworks: Perspective and Suggestions for Future Research. *ACS Catal.* **2019,** *9*, 1779-1798.

(4) Shearer, G. C.; Chavan, S.; Bordiga, S.; Svelle, S.; Olsbye, U.; Lillerud, K. P., Defect Engineering: Tuning the Porosity and Composition of the Metal-Organic Framework UiO-66 via Modulated Synthesis. *Chem. Mater.* **2016,** *28*, 3749-3761.

(5) Yang, D.; Ortuno, M. A.; Bernales, V.; Cramer, C. J.; Gagliardi, L.; Gates, B. C., Structure and Dynamics of Zr_6O_8 Metal-Organic Framework Node Surfaces Probed with Ethanol Dehydration as a Catalytic Test Reaction. *J. Am. Chem. Soc.* **2018,** *140*, 3751-3759.

(6) Wei, R.; Gaggioli, C. A.; Li, G.; Islamoglu, T.; Zhang, Z.; Yu, P.; Farha, O. K.; Cramer, C. J.; Gagliardi, L.; Yang, D.; Gates, B. C., Tuning the Properties of Zr_6O_8 Nodes in the Metal Organic Framework UiO-66 by Selection of Node-Bound Ligands and Linkers. *Chem. Mater.* **2019,** *31*, 1655-1663.

(7) Vermoortele, F.; Bueken, B.; Le Bars, G.; Van de Voorde, B.; Vandichel, M.; Houthoofd, K.; Vimont, A.; Daturi, M.; Waroquier, M.; Van Speybroeck, V.; Kirschhock, C.; De Vos, D. E., Synthesis Modulation as a Tool To Increase the Catalytic Activity of Metal-Organic Frameworks: The Unique Case of UiO-66(Zr). *J. Am. Chem. Soc.* **2013,** *135*, 11465-11468.

(8) Mondloch, J. E.; Katz, M. J.; Isley, W. C.; Ghosh, P.; Liao, P. L.; Bury, W.; Wagner, G.; Hall, M. G.; DeCoste, J. B.; Peterson, G. W.; Snurr, R. Q.; Cramer, C. J.; Hupp, J. T.; Farha, O. K., Destruction of Chemical Warfare Agents Using Metal-Organic Frameworks. *Nat. Mater.* **2015,** *14*, 512-516.

(9) Yang, D.; Odoh, S. O.; Borycz, J.; Wang, T. C.; Farha, O. K.; Hupp, J. T.; Cramer, C. J.; Gagliardi, L.; Gates, B. C., Tuning Zr_6 Metal-Organic Framework (MOF) Nodes as Catalyst Supports: Site Densities and Electron-Donor Properties Influence Molecular Iridium Complexes as Ethylene Conversion Catalysts. *ACS Catal.* **2016,** *6*, 235-247.

(10) Yang, D.; Odoh, S. O.; Wang, T. C.; Farha, O. K.; Hupp, J. T.; Cramer, C. J.; Gagliardi, L.; Gates, B. C., Metal-Organic Framework Nodes as Nearly Ideal Supports for Molecular Catalysts: NU-1000-and UiO-66-Supported Iridium Complexes. *J. Am. Chem. Soc.* **2015,** *137*, 7391-7396.

(11) Yuan, S.; Chen, Y. P.; Qin, J. S.; Lu, W. G.; Wang, X.; Zhang, Q.; Bosch, M.; Liu, T. F.; Lian, X. Z.; Zhou, H. C., Cooperative Cluster Metalation and Ligand Migration in Zirconium Metal-Organic Frameworks. *Angew. Chem., Int. Ed.* **2015,** *54*, 14696-14700.

(12) Wu, H.; Chua, Y. S.; Krungleviciute, V.; Tyagi, M.; Chen, P.; Yildirim, T.; Zhou, W., Unusual and Highly Tunable Missing-Linker Defects in Zirconium Metal-Organic Framework UiO-66 and Their Important Effects on Gas Adsorption. *J. Am. Chem. Soc.* **2013,** *135*, 10525-10532.

(13) Cliffe, M. J.; Wan, W.; Zou, X. D.; Chater, P. A.; Kleppe, A. K.; Tucker, M. G.; Wilhelm, H.; Funnell, N. P.; Coudert, F. X.; Goodwin, A. L., Correlated Defect Nanoregions in a Metal-Organic Framework. *Nat. Commun.* **2014,** *5*, No. 4176.

(14) Cheetham, A. K.; Bennett, T. D.; Coudert, F. X.; Goodwin, A. L., Defects and Disorder in Metal Organic Frameworks. *Dalton Trans.* **2016,** *45*, 4113-4126.

(15) Dissegna, S.; Epp, K.; Heinz, W. R.; Kieslich, G.; Fischer, R. A., Defective Metal-Organic Frameworks. *Adv. Mater.* **2018,** *30*, 1704501.

(16) Fang, Z. L.; Bueken, B.; De Vos, D. E.; Fischer, R. A., Defect-Engineered Metal-Organic Frameworks. *Angew. Chem., Int. Ed.* **2015,** *54*, 7234-7254.

(17) Liu, Y. Y.; Klet, R. C.; Hupp, J. T.; Farha, O., Probing the Correlations between the Defects in Metal-Organic Frameworks and their Catalytic Activity by an Epoxide Ring-Opening Reaction. *Chem. Commun.* **2016,** *52*, 7806-7809.

(18) Cliffe, M. J.; Castillo-Martinez, E.; Wu, Y.; Lee, J.; Forse, A. C.; Firth, F. C. N.; Moghadam, P. Z.; Fairen-Jimenez, D.; Gaultois, M. W.; Hill, J. A.; Magdysyuk, O. V.; Slater, B.; Goodwin, A. L.; Grey, C. P., Metal-Organic Nanosheets Formed via Defect-Mediated Transformation of a Hafnium Metal-Organic Framework. *J. Am. Chem. Soc.* **2017,** *139*, 5397-5404.

(19) Bezrukov, A. A.; Tornroos, K. W.; Le Roux, E.; Dietzel, P. D. C., Incorporation of an Intact Dimeric Zr_{12} oxo Cluster from a Molecular Precursor in a New Zirconium Metal-Organic Framework. *Chem. Commun.* **2018,** *54*, 2735-2738.

(20) Peh, S. B.; Cheng, Y.; Zhang, J.; Wang, Y.; Chan, G. H.; Wang, J.; Zhao,

D., Cluster Nuclearity Control and Modulated Hydrothermal Synthesis of Functionalized Zr_{12} Metal-Organic Frameworks. *Dalton Trans.* **2019,** *48*, 7069-7073.

(21) Ji, P.; Manna, K.; Lin, Z.; Feng, X.; Urban, A.; Song, Y.; Lin, W., Single-Site Cobalt Catalysts at New $Zr_{12}(\mu_3\text{-}O)_8(\mu_3\text{-}OH)_8(\mu_2\text{-}OH)_6$ Metal-Organic Framework Nodes for Highly Active Hydrogenation of Nitroarenes, Nitriles, and Isocyanides. *J. Am. Chem. Soc.* **2017,** *139*, 7004-7011.

(22) Ermer, M.; Mehler, J.; Kriesten, M.; Avadhut, Y. S.; Schulz, P. S.; Hartmann, M., Synthesis of the Novel MOF **hcp** UiO-66 Employing Ionic Liquids as a Linker Precursor. *Dalton Trans.* **2018,** *47*, 14426-14430.

(23) Firth, F. C. N.; Cliffe, M. J.; Vulpe, D.; Aragones-Anglada, M.; Moghadam, P. Z.; Fairen-Jimenez, D.; Slater, B.; Grey, C. P., Engineering New Defective Phases of UiO Family Metal-Organic Frameworks with Water. *J. Mater. Chem. A* **2019,** *7*, 7459-7469.

(24) Hennig, C.; Weiss, S.; Kraus, W.; Kretzschmar, J.; Scheinost, A. C., Solution Species and Crystal Structure of Zr(IV) Acetate. *Inorg. Chem.* **2017,** *56*, 2473-2480.

(25) Butova, V. V.; Budnyk, A. P.; Charykov, K. M.; Vetlitsyna-Novikova, K. S.; Lamberti, C.; Soldatov, A. V., Water as a Structure-Driving Agent between the UiO-66 and MIL-140A Metal-Organic Frameworks. *Chem. Commun.* **2019,** *55*, 901-904.

(26) Yang, D.; Bernales, V.; Islamoglu, T.; Farha, O. K.; Hupp, J. T.; Cramer, C. J.; Gagliardi, L.; Gates, B. C., Tuning the Surface Chemistry of Metal Organic Framework Nodes: Proton Topology of the Metal-Oxide-Like Zr_6 Nodes of UiO-66 and NU-1000. *J. Am. Chem. Soc.* **2016,** *138*, 15189-15196.

(27) Momeni, M. R.; Cramer, C. J., Structural Characterization of Pristine and Defective $[Zr_{12}(\mu_3\text{-}O)_8(\mu_3\text{-}OH)_8(\mu_2\text{-}OH)_6]^{18+}$ Double-Node Metal-Organic Framework and Predicted Applications for Single-Site Catalytic Hydrolysis of Sarin. *Chem. Mater.* **2018,** *30*, 4432-4439.

(28) Valenzano, L.; Civalleri, B.; Chavan, S.; Bordiga, S.; Nilsen, M. H.; Jakobsen, S.; Lillerud, K. P.; Lamberti, C., Disclosing the Complex Structure of UiO-66 Metal Organic Framework: A Synergic Combination of Experiment and Theory. *Chem. Mater.* **2011,** *23*, 1700-1718.

(29) Jiang, J. C.; Gandara, F.; Zhang, Y. B.; Na, K.; Yaghi, O. M.; Klemperer, W. G., Superacidity in Sulfated Metal-Organic Framework-808. *J. Am. Chem. Soc.* **2014,** *136*, 12844-12847.

(30) Garcia-Garcia, P.; Muller, M.; Corma, A., MOF Catalysis in Relation to their Homogeneous Counterparts and Conventional Solid Catalysts. *Chem. Sci.* **2014,** *5*, 2979-3007.

(31) Beyzavi, M. H.; Klet, R. C.; Tussupbayev, S.; Borycz, J.; Vermeulen, N. A.; Cramer, C. J.; Stoddart, J. F.; Hupp, J. T.; Farha, O. K., A Hafnium-Based Metal Organic Framework as an Efficient and Multifunctional Catalyst for Facile CO_2 Fixation and Regioselective and Enantioretentive Epoxide Activation. *J. Am. Chem. Soc.* **2014,** *136*, 15861-15864.

(32) Jung, K. T.; Bell, A. T., An In Situ Infrared Study of Dimethyl Carbonate Synthesis from Carbon Dioxide and Methanol over Zirconia. *J. Catal.* **2001,** *204*, 339-347.

(33) Pourfarzad, A.; Ahmadian, Z.; Habibi-Najafi, M. B., Interactions between Polyols and Wheat Biopolymers in a Bread model System Fortified with Inulin: A Fourier Transform Infrared Study. *Heliyon* **2018**, *4*, e01017.

(34) Dhakshinamoorthy, A.; Alvaro, M.; Concepcion, P.; Fornes, V.; Garcia, H., Graphene Oxide as an Acid Catalyst for the Room Temperature Ring Opening of Epoxides. *Chem. Commun.* **2012**, *48*, 5443-5445.

(35) Blandez, J. F.; Santiago-Portillo, A.; Navalon, S.; Gimenez-Marques, M.; Alvaro, M.; Horcajada, P.; Garcia, H., Influence of Functionalization of Terephthalate Linker on the Catalytic Activity of UiO-66 for Epoxide Ring Opening. *J. Mol. Catal. A* **2016**, *425*, 332-339.

(36) Vermoortele, F.; Vandichel, M.; Van de Voorde, B.; Ameloot, R.; Waroquier, M.; Van Speybroeck, V.; De Vos, D. E., Electronic Effects of Linker Substitution on Lewis Acid Catalysis with Metal-Organic Frameworks. *Angew. Chem., Int. Ed.* **2012,** *51*, 4887-4890.

(37) Katz, M. J.; Moon, S. Y.; Mondloch, J. E.; Beyzavi, M. H.; Stephenson, C. J.; Hupp, J. T.; Farha, O. K., Exploiting Parameter Space in MOFs: A 20-Fold Enhancement of Phosphate-Ester Hydrolysis with UiO-66-NH_2. *Chem. Sci.* **2015,** *6*, 2286-2291.

(38) Islamoglu, T.; Ortuno, M. A.; Proussaloglou, E.; Howarth, A. J.; Vermeulen, N. A.; Atilgan, A.; Asiri, A. M.; Cramer, C. J.; Farha, O. K., Presence versus Proximity: The Role of Pendant Amines in the Catalytic Hydrolysis of a Nerve Agent Simulant. *Angew. Chem., Int. Ed.* **2018,** *57*, 1949-1953.

TOC